RAA 2020 Vol. **20** No. **8**, 132(9pp) doi: 10.1088/1674–4527/20/8/132

http://www.raa-journal.org *http://iopscience.iop.org/raa*

Research in Astronomy and Astrophysics

Thermodynamic model of comet 29P/SW brightness changing

Marcin Wesołowski

College of Natural Sciences, Institute of Physics, University of Rzeszów, Pigonia 1 Street, 35-310 Rzeszów, Poland; *marwes@ur.edu.pl*

Received 2020 February 13; accepted 2020 March 25

Abstract We analyze the thermodynamic model of changes in comet brightness focusing on the exceptional case which is comet 29P/Schwassmann-Wachmann (hereafter 29P/SW). This object demonstrates quasi-regular flares that occur in a short period of time; most often it lasts about a dozen hours. The analysis of observational data shows that the average number of comet outbursts for 29P/SW is 7.3 per year. This is the only known comet with such a number of outbursts per year, which demonstrates its uniqueness. In the proposed approach to analyze the outburst of comet 29P/SW, we took into account the complex structure of particles which are in its coma and assumed that they are composed of water ice, dust and organic matter. The paper explains how this diversity affects the more efficient scattering of incident sunlight during the outburst of comet 29P/SW.

Key words: comets: general — comets: individual: 29P/Schwassmann-Wachmann

1 INTRODUCTION

Comet 29P/Schwassmann-Wachmann (29P/SW) was discovered in 1927, most likely during one of its numerous outbursts. It is characterized by two main features that are associated with its orbit and the frequency of outbursts (statistically 7.3 per year, Ivanova et al. 2012). Comet 29P/SW is moving in an almost circular orbit with an eccentricity equal to $e = 0.0441$ and semi-major axis $a = 5.986\,\mathrm{au} \approx 6\,\mathrm{au}$. This means that it moves between the orbits of Jupiter and Saturn. Comparing comet 29P/SW with other comets, one can notice two main differences. First, the nucleus size is estimated to be $60.4 \pm 7.4\,\mathrm{km}$ (Schambeau et al. 2015), and second, it is characterized by a long rotation period of about $P = 60\,\mathrm{d}$ (Miles 2016).

The outburst of comet brightness is among the most spectacular phenomena that can be observed in the night sky. Despite plenty of observations carried out during many years as well as the efforts of theorists, the puzzle of comet brightness has not been fully resolved. However, there is a kind of consensus among researchers that comet outbursts are caused mainly by rapid emission of gas and dust into its coma.

Other features of outbursts of 29P/SW are (Richter 1954; Hughes 1991; Gronkowski & Wesołowski 2015):

- the mass of ejected material ranges from 10^8 kg to 10^9 kg,
- the energy released during outburst ranges from 10^{12} J to 10^{16} J,
- this energy is associated with expansion of the coma,
- the expansion of the coma occurs at a speed of about $100 - 400\,\mathrm{m\,s^{-1}}$,
- the density of matter in a coma decreases when the distance from the nucleus increases,
- the spectrum of comet flare is continuous,
- the brightness of the comet in the quiet phase is $15 - 16$ mag,
- the brightness of the comet in the outburst phase is $13 - 11$ mag,
- the time to return to quiet phase is about several days (ranging from 20 to 30 d, on average).

Note that so far no significant changes in the comet's orbital parameters have been observed due to the changes in their brightness.

Considering the similarities and differences between the outbursts of comet 29P/SW and those of other comets (e.g., 1P/Halley or 17P/Holmes, etc.), we conclude that the course of events is practically the same. The difference in their outbursts is related mainly to the magnitude of brightness changes. It is worth noting that in order to determine the brightness changes of comets, it is important to take into account the heliocentric distances as well as the sublimation activity of a type of cometary ice.

Another issue that causes some difficulties in the actual assessment of brightness of a given astronomical object can be the observational conditions, that is to say the ‘quality of the sky’, i.e., the degree of its artificial light pollution (Gronkowski et al. 2018; Wesołowski 2019).

The main aim of the paper is to explain how the diversity of particles (in terms of their structure and size) affects the more efficient scattering of incident sunlight during the outburst of comet 29P/SW. In the paper, the complex structure of cometary particles consisting of water ice, organic matter and dust is taken into account. Their percentage in the coma was also analyzed and how it affects the brightness of comet 29P/SW is explained. For this purpose, a thermodynamic cometary outburst model is applied.

2 SELECTED MECHANISMS OF THE BRIGHTNESS OUTBURSTS

Up to now, in the scientific literature many different mechanisms that can explain this phenomenon have been proposed. The most frequently discussed nowadays are:

- the pressure mechanism,
- the collision mechanism,
- the solar wind,
- the polymerization of hydrogen cyanide (HCN),
- the transformation of crystalline to amorphous ice,
- the existence of cavities within the comet,
- the melting of cometary ice,
- the cryovolcanoes.

The models listed above were already discussed in numerous papers (Hughes 1991; Enzian et al. 1997; Gronkowski & Wesołowski 2012, 2015, 2016; Wesołowski & Gronkowski 2018a). Analyzing these hypotheses, we find that none of them fully explain all the morphological features of cometary outbursts. However, the mechanisms mentioned above clearly hypothesize that one of the main causes of comet outbursts is the ejection of some part of the nucleus material into outer space. Nevertheless, despite the progress that has been made so far, the problem of comet outbursts remains open.

3 COMET 29P/SW CHANGES IN BRIGHTNESS

As was already mentioned above, the outbursts are associated with the ejection of material from the comet’s nucleus. This material comes from the destruction of a fragment on the surface of the comet’s nucleus. In what follows, we do not try to answer the question of what mechanisms or their combination are responsible for the outburst, but rather we consider the changes in comet brightness using thermodynamic arguments. The calculations performed demonstrate the relationship between the change in brightness as a function of the mass ejected. In order to obtain a more detailed description of the outburst, we examine how cometary particles made of water ice, dust or organic matter affect the range of jump in comet brightness. The diversity of structure and sizes of ejected material particles was observed by the *Rosetta* mission to comet 67P/Churyumov-Gerasimenko (hereafter 67P/Ch-G).

It should be clearly stated that the source of sunlight reflection by coma is the particles which are present in it. Studying the physical properties of cometary particles has a long history. It is very probable that water ice in crystalline or amorphous form is the main component of cometary nuclei. It is assumed that ice particles with an admixture of dark material have to be present in the atmospheres of comets in significant amounts. This is confirmed both by observations (Kawakita et al. 2004), as well as by theoretical studies (Beer et al. 2006, 2008). On the other hand, both laboratory tests as well as the results of space missions, especially the *Rosetta* mission, have demonstrated that cometary particles may have a complex, fragile structure of agglomerates composed of submicron monomers. The analysis of measurements carried out by the test instruments onboard the *Rosetta* probe allows us to distinguish the following families of cometary particles: Ballistic Aggregates, Ballistic Aggregates Type 1, Ballistic Aggregates Type 2 and Ballistic Cluster-Cluster Aggregates (see: Skorov et al. 2016). It should be expected that, in accordance with one of the possible mechanisms, at a gentle sublimation from the comet surface, particles can be ejected into the coma both in the form of ice crumbs and in the form of agglomerates. On the other hand, during the outburst of the comet’s brightness, some part of the nucleus’ surface layer can be ejected, probably in the form of debris of cometary material. Therefore, in the numerical calculations we take into account not only water ice, but also the dust and organic matter, because they are all responsible for the agglomerates to appear. We assume the agglomerates are composed of monomers (their average size is about 0.1 μm), while the size of the agglomerates is assumed to be about a few centimeters (Wesołowski et al. 2020b).

However, when it comes to comet matter, it is worth noting that many authors who dealt with it considered irregular shapes of dust particles and various levels of porosity in them. In their papers, numerical calculations were done applying Discrete Dipole Approximation or T-Matrix theory (see e.g., Mishchenko et al. 1996; Kolokolova et al. 2004; Zubko et al. 2011). These two methods are very accurate but complicated and very time consuming. In order to determine the effective scattering cross-section for spheres of dirty water ice-grains, we implement a method based on Lorentz-Mie theory. However, to determine the analogous characteristics for aggregates containing silicate monomers, we use the results of relevant calculations based on the Discrete Dipole Approximation theory and presented by Zubko (2013).

The first step in a way to understand the physical processes related to cometary outbursts is choice of an adequate model for the thermodynamic evolution of the comet's nucleus. In the case of comet 29P/SW, we assume that sublimation activity is dominated by carbon monoxide sublimation occurring from the interior of the comet's nucleus. In what follows, we utilize the energy balance equation on the surface of the nucleus having the form

$$\frac{S_{\odot}(1-A_{\mathrm{N}})\cos\varphi}{R_{\mathrm{H}}^{2}} = \epsilon\,\sigma\,T^{4} + f\,\frac{\dot{Z}\,L(T)}{N_{\mathrm{A}}} + h(\psi)\,K(T)\,\nabla T. \tag{1}$$

In this equation, the left side stands for the solar radiation energy absorbed by the nucleus, the right side is a sum of what is reradiated by nucleus energy, the energy consumed for the sublimation of cometary ice and the heat conducted into the interior of the cometary nucleus. The following notation is adopted: $S_{\odot}$ - the solar constant at heliocentric distance, A_{N} - the albedo, φ - the angle between the normal to the surface of the nucleus and the direction to the Sun, R_{H} - the heliocentric distance of the comet, ϵ - the infrared emissivity of the nucleus, σ - the Stefan-Boltzmann constant, $\dot{Z}$ - the rate of cometary ice sublimation (expressed in molecules $\mathrm{m^{-2}s^{-1}}$, $L(T)$ - the latent heat of sublimation of cometary material and N_{A} - Avogadro's number. Parameter $K(T)$ stands for the average heat conductivity of a comet nucleus which is a function of temperature T. The heat conductivity $K(T)$ is corrected by a Hertz factor $h(\psi)$ in order to take into account porosity ψ, as was done in Tancredi et al. (1994); Davidsson & Skorov (2002), because in case of significant porosity the contact surface between cometary particles becomes smaller.

In order to correctly describe the sublimation occurring from the surface and subsurface layers of the nucleus, the following three processes should be taken into account: evaporation, condensation and the outflow of comet matter through the porous nucleus. These processes can be described by the following equations (Gronkowski & Wesołowski 2015):

$$n_{\mathrm{ev}} = \frac{f p_{\mathrm{s}}}{\sqrt{2\pi m k T}}, \tag{2}$$

$$n_{\mathrm{ab}} = \frac{\alpha p}{\sqrt{2\pi m k T}}, \tag{3}$$

$$n_{\mathrm{sub}} = \sum_{\mathrm{i}} (n_{\mathrm{ev}} - n_{\mathrm{ab}}), \tag{4}$$

$$J = -\frac{16}{3}\sqrt{\frac{\mu}{2\pi R_{\mathrm{g}}}}\,\Phi\,(\psi,r)\,\frac{\mathrm{d}}{\mathrm{d}x}\left(\frac{p}{\sqrt{T}}\right), \tag{5}$$

$$n_{\mathrm{esc}} = \sum_{\mathrm{i}} \frac{|J_{\mathrm{i}}|}{m_{\mathrm{i}}}. \tag{6}$$

Equation (2) expresses the rate of cometary ice evaporation n_{ev}. Here f, p_{s}, m, k and T denote the fraction of the surface which exhibits sublimation activity of cometary ice, its saturated vapor pressure and the molecular mass, the Boltzmann constant and temperature, respectively. Equation (3) describes the rate of cometary ice condensation, and α and p represent its condensation (or sticking) coefficient and pressure, respectively. Equation (4) stands for the total net rate of sublimation n_{sub} expressed in terms of molecules $\mathrm{m^{-2}s^{-1}}$. The total outflow of cometary ice (in $\mathrm{kg\,m^{-2}s^{-1}}$ units) is given by Equation (5). Here μ represents the molecular weight of cometary ice and R_{g} denotes the universal gas constant. Equation (6) expresses the same flux n_{esc} but in units of molecules $\mathrm{m^{-2}s^{-1}}$. The saturated vapor pressure for CO is given by the following formula (Fanale & Salvail 1990)

$$p_{\mathrm{s,CO}} = 1.6624\cdot 10^{9}\exp(-764.16/T). \tag{7}$$

Equations (1)–(7) determine the thermodynamic conditions prevailing in the structure of the comet's nucleus. Using them, one can determine the amplitude of the comet's brightness change applying Pogson's law (Gronkowski et al. 2018; Wesołowski & Gronkowski 2018a; Wesołowski & Gronkowski 2018b; Wesołowski 2019; Wesołowski et al. 2020b). In general form, Pogson's law is given by the following relation

$$\Delta m = -2.5\log\frac{p(\theta)(t_2)\,(C_{\mathrm{Scat}}(t_2)+C_{\mathrm{Scat}}(M_{\mathrm{ej}}))}{p(\theta)(t_1)C_{\mathrm{Scat}}(t_1)}, \tag{8}$$

where $p(\theta)(t_1)$ is the value of the phase function (see below) during the quiet sublimation and $p(\theta)(t_2)$ is the value of phase function during the outburst. The analysis of individual scattering cross-sections was presented in Wesołowski & Gronkowski (2018a). Here, we restrict our description to only the final formula for the total scattering cross-section for cometary particles

$$C_{\mathrm{Scat}}(t_{\mathrm{i}}) = \pi N_{\mathrm{particles}}(t_{\mathrm{i}}) \times \int_{r_{\mathrm{min}}}^{r_{\mathrm{max}}} Q(\lambda,x_{\mathrm{eff}},m) r^2 h(r) dr. \tag{9}$$

The individual symbols written in Equation (9) are: $Q(\lambda, x_{\mathrm{eff}}, m)$ - the scattering efficiencies of cometary particles, $h(r)$ - their size distribution function, index $i = 1$ refers to the phase of quiet sublimation, $i = 2$ signifies the phase of outburst, λ is the wavelength of electromagnetic solar radiation, x_{eff} - the effective diffraction parameter and m - the effective index of grain material which is a complex number. The diffraction parameter can be determined by the following formula

$$x_{\mathrm{eff}} = \frac{2\pi}{\lambda} r_{\mathrm{eff}} = \frac{2\pi \int_{r_{\min}}^{r_{\max}} r^{-2.7} dr}{\lambda \int_{r_{\min}}^{r_{\max}} r^{-3.7} dr}. \tag{10}$$

This formula is a consequence of the adopted distribution function (Lin et al. 2017)

$$h(r) = C \cdot r^{-3.7}, \tag{11}$$

where r and C are the radius of the effective cross-section of fluffy aggregate and the normalization constant, respectively.

The scattering efficiency was calculated here in the framework of Mie theory. The value of wavelength λ scattered by the particles in a coma is determined by Wien's law. The parameter $C_{\mathrm{Scat}}(M_{\mathrm{ej}})$ in Equation (8) is the total scattering cross-section resulting from the destruction of a nucleus layer fragment. The value of this parameter determined by the amount of mass ejected from the nucleus surface and is calculated by means of the following formula

$$M_{\mathrm{ej}} = 4\pi h \rho_{\mathrm{particles}} R_{\mathrm{N}}^2 \left(\eta(t_2) - \eta(t_1)\right), \tag{12}$$

where h is the thickness of the layer that has been destroyed, $\rho_{\mathrm{particles}}$ is the particle density and R_{N} is the radius of the cometary nucleus. The symbols $\eta(t_1)$ and $\eta(t_2)$ denote a fraction of the surface that is active in the calm sublimation phase and during the outburst, respectively.

In Equation (8) there is an important factor, namely phase function $p(\theta)$, which represents the probability of a photon being scattered at the angle θ. The value of $p(\theta)$ depends on the angle θ which is the angle between the lines connecting, on one hand, the observer and Sun and, on the other hand, the Sun and comet (see Fig. 1). The angle θ is determined by the formula

– at perihelion:

$$\theta_{\mathrm{q}} = \arcsin \frac{\mathrm{r_E}}{\mathrm{r_q}}, \tag{13}$$

– at aphelion:

$$\theta_{\mathrm{Q}} = \arcsin \frac{\mathrm{r_E}}{\mathrm{r_Q}}. \tag{14}$$

In our case, we assume that the outburst of comet 29P/SW occurs at the perihelion of its orbit ($R_{\mathrm{q}} = 5.722$ au); then the phase angle is $\Theta_{\mathrm{q}} = 10.06°$. At the aphelion of the comet's orbit ($R_{\mathrm{Q}} = 6.25$ au) the value of this angle is $\Theta_{\mathrm{Q}} = 9.21°$. The phase function $p(\Theta)$ in Equation (8) describes the angular distribution of radiation scattered by cometary particles. For particle sizes comparable to the radiation wavelength, the Henyey-Greenstein model is employed most often. The phase function in this case is parameterized by the asymmetry coefficient g, which results from the following expression

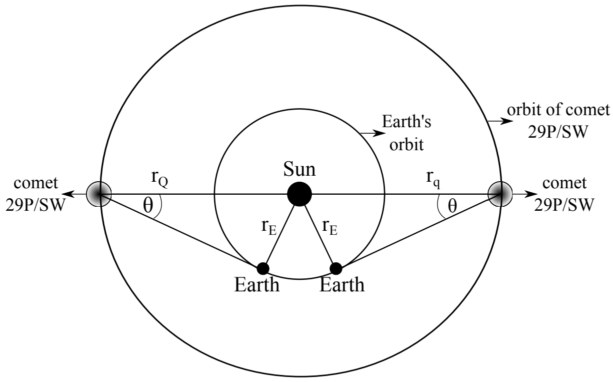

Fig. 1 Here the individual symbols mean: θ - the phase angle, r_{q} - the distance between the comet and the Sun when the comet is at perihelion, r_{Q} - the distance between the comet and Sun when the comet is at aphelion and r_{E} - the distance of Earth from the Sun ($r_{\mathrm{E}} = 1$ au).

$$g = \frac{2\sum_{n=1}^{\infty}\left(\frac{n(n+2)}{n+1}\mathrm{Re}(a_{\mathrm{n}}a_{\mathrm{n+1}}^{*} + b_{\mathrm{n}}b_{\mathrm{n+1}}^{*}) + \frac{2n+1}{n(n+1)}\mathrm{Re}(a_{\mathrm{n}}b_{\mathrm{n}}^{*})\right)}{\sum_{n=1}^{\infty}(2n+1)(|a_{\mathrm{n}}|^2 + |b_{\mathrm{n}}|^2)}, \tag{15}$$

where the asterisk (superscript) denotes complex conjugate. Therefore, the formula which determines the phase function is

$$p(\theta) = \frac{(1-g^2)}{4\pi\left(1+g^2-2g\cdot\cos(\theta)\right)^{3/2}}. \tag{16}$$

Using Equations (1)–(16), one can express the next formula through Pogson's law

$$\Delta m = -2.5 \log \frac{p(\theta)_{\mathrm{ice}}\left(C_{\mathrm{ice}}(t_2) + C_{\mathrm{ej,ice}}\right) + p(\theta)_{\mathrm{dust}}C_{\mathrm{ej,dust}} + p(\theta)_{\mathrm{org}}C_{\mathrm{ej,org}}}{p(\theta)_{\mathrm{ice}}C_{\mathrm{ice}}(t_1)}. \tag{17}$$

The individual scattering cross-sections occurring in Equation (17) can be written as:

$$C_{\mathrm{ice}}(t_i) = \frac{3\pi\eta(t_{\mathrm{i}})\kappa R_{\mathrm{N}}^2 \dot{Z} R_{\mathrm{h}}(t_{\mathrm{i}}) m_{\mathrm{g}} \int_{\mathrm{r_{min}}}^{\mathrm{r_{max}}} Q_{\mathrm{ice}} r^2 h(r) dr}{v_{\mathrm{g}}\rho_{\mathrm{ice}} \int_{\mathrm{r_{min}}}^{\mathrm{r_{max}}} r^3 h(r) dr}, \tag{18}$$

$$C_{\mathrm{ej,ice}} = \frac{3M_{\mathrm{ej,ice}} \int_{\mathrm{r_{min}}}^{\mathrm{r_{max}}} Q_{\mathrm{ice}} r^2 h(r) dr}{4\rho_{\mathrm{ice}} \int_{\mathrm{r_{min}}}^{\mathrm{r_{max}}} r^3 h(r) dr}, \tag{19}$$

$$C_{\mathrm{ej,dust}} = \frac{3M_{\mathrm{ej,dust}} \int_{\mathrm{r_{min}}}^{\mathrm{r_{max}}} Q_{\mathrm{dust}} r^2 h(r) dr}{4\rho_{\mathrm{dust}} \int_{\mathrm{r_{min}}}^{\mathrm{r_{max}}} r^3 h(r) dr}, \tag{20}$$

and

$$C_{\mathrm{ej,org}} = \frac{3M_{\mathrm{ej,org}} \int_{\mathrm{r_{min}}}^{\mathrm{r_{max}}} Q_{\mathrm{org}} r^2 h(r) dr}{4\rho_{\mathrm{org}} \int_{\mathrm{r_{min}}}^{\mathrm{r_{max}}} r^3 h(r) dr}. \tag{21}$$

Here Q_{ice}, Q_{dust} and Q_{org} stand for the scattering efficiencies of ice water particles, dust particles and organic

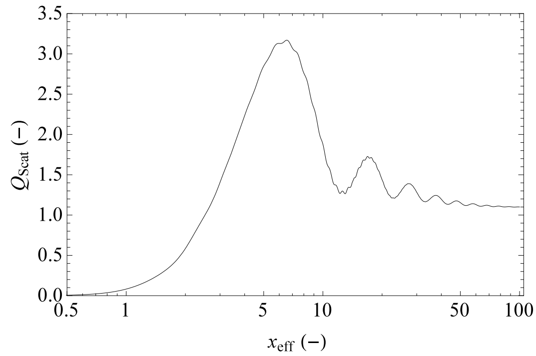

Fig. 2 The scattering efficiencies of cometary particles containing water ice with refractive index $m_{\rm ice} = 1.31 + 0.02i$ as a function of diffraction parameter.

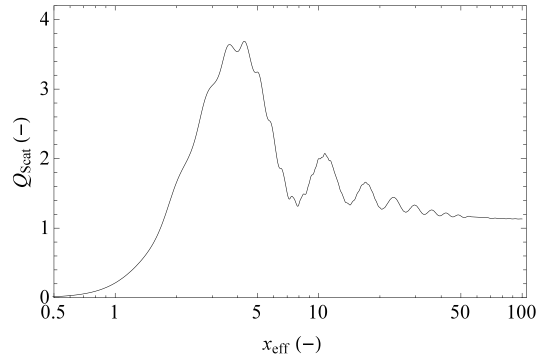

Fig. 3 Similar to Fig. 2, but calculations were carried out for cometary dust with refractive index $m_{\rm dust} = 1.60 + 0.02i$.

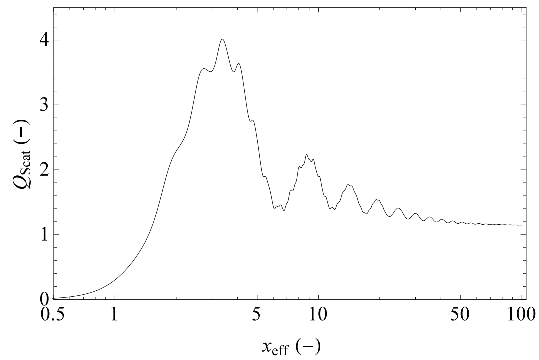

Fig. 4 Similar to Fig. 2, but calculations were carried out for organic matter with refractive index $m_{\rm dust} = 1.50 + 0.02i$.

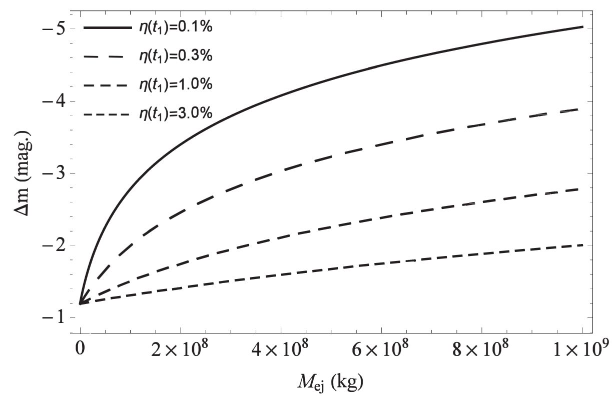

Fig. 5 The jump in comet 29P/SW brightness Δm as a function of ejected mass $M_{\rm ej}$ for different values of parameter $\eta(\rm t_1)$. It is assumed that the comet is at perihelion in its orbit ($R_{\rm H} = 5.722$ au), and its activity is controlled by sublimation of carbon monoxide. It is also assumed that light scattering is due to water ice particles.

matter, respectively. The other symbols are κ is the dust-gas mass ratio, $\dot{Z}$ is the rate of sublimation for cometary ice, $R_{\rm h}(t_{\rm i})$ - radius of the cometary coma in the gentle and outburst phase, $m_{\rm g}$ - the mass of cometary gas, $\rho_{\rm gr}$ - the density of ice particles, $\rho_{\rm dust}$ - the density of dust, $\rho_{\rm org}$ - the density of organic matter and $v_{\rm g}$ - the mean radial velocity of gas molecules.

4 RESULTS

The physical parameters taken into account in the simulations are listed in Table 1, while their results are presented below. In Figures 2–4, the distribution of the scattering factor as a function of size parameter (parameter diffraction) for these three cometary materials is shown. In the calculations, three types of cometary materials were taken into account: water ice, dust and organic matter. We also assume that ejected cometary material forms a cloud of spherical ice-dust grains as well as agglomerates of silicate monomers. Then, we can directly apply the Lorentz-Mie theory to the first type of particle, while for the second type of particle, the results are obtained by Zubko (2013) by means of Discrete Dipole Approximation. The results of numerical simulations are presented in Figures 5–15. In each of these cases, the percentage of considered cometary material is different. The results of our calculations related to the comet 29P/SW are in accordance with the results reported by observers.

5 SUMMARY AND CONCLUSIONS

The outburst activity of comet 29P/SW is a very intriguing issue in modern cometary science. There have been some attempts which were trying to explain this issue. The thermodynamic model presented in this paper takes into account the main morphological features that are observed during the comet's outburst and for this reason this model seems to be interesting and attractive. It is worth emphasizing that the obtained results are consistent with the observations of comet 29P/SW during its outbursts.

When studying the outburst of comet 29P/SW using the thermodynamic model, the key parameter is the surface temperature of the nucleus as well as the temperature

Table 1 Values of Cometary Parameters used in the Numerical Simulations

Parameter	Value(s)	Reference
Albedo (-)	$A_{\rm N} = 0.024$	Stansberry et al. (2004)
Density of the cometary nucleus (kg m^{-3})	$\rho_{\rm N} = 400$	Richardson et al. (2007)
Density of ice particles (kg m^{-3})	$\rho_{\rm ice} = 920$	Reach et al. (2010)
Density of cometary dust (kg m^{-3})	$\rho_{\rm dust} = 3000$	Laor & Draine (1993)
Density of organic matter (kg m^{-3})	$\rho_{\rm org} = 1500$	Wesołowski et al. (2020a)
Crystalline ice thermal conductivity (W m^{-1} K^{-1})	$\lambda_{\rm core}(T) = 567/T$	Enzian et al. (1997)
Dust conductivity (W m^{-1} K^{-1})	$\lambda_{\rm dust}(T) \approx 2$	Enzian et al. (1997)
Initial temperature (K)	$T = 50$	Kossacki & Szutowicz (2008)
Hertz factor (-)	$h(\psi) = 0.01$	Kossacki & Szutowicz (2013)
Porosity (-)	$\psi = 0.7$	Kossacki & Szutowicz (2013)
Dust - gas mass ratio (-)	$\kappa = 1$	Gronkowski & Wesołowski (2015)
Emissivity (-)	$\epsilon = 0.9$	Wesołowski et al. (2019)
Depth of cavity location (m)	$\Delta x = 10$	Meech et al. (2009)
Constant $A_{\rm CO}$ for carbon monoxide (Pa)	$A_{\rm CO} = 1.6624 \times 10^9$	Fanale & Salvail (1990)
Constant $B_{\rm CO}$ for carbon monoxide (K)	$B_{\rm CO} = 764.16$	Fanale & Salvail (1990)
Latent heat of carbon monoxide sublimation (J kg^{-1})	$L(T)_{\rm CO} = 2.93 \times 10^5$	Enzian et al. (1997)
Radius of cometary coma during the outburst (m)	$R_{\rm h}(t_2) = 3{\times}10^8$	Hughes (1991)
Radius of the cometary coma during gentle sublimation (m)	$R_{\rm h}(t_1) = 1{\times}10^8$	Hughes (1991)
Minimum radius of cometary particles (m)	$r_{\rm min} = 10^{-7}$	Gronkowski & Wesołowski (2015)
Maximum radius of cometary particles (m)	$r_{\rm max} = 10^{-2}$	Gronkowski & Wesołowski (2015)
Solar constant (for d = 1 au) (W m^{-2})	$S_{\odot} = 1360.8 \pm 0.5$	Kopp & Lean (2011)
Mean value of solar radiation wavelength (m)	$\lambda = 0.5015 \times 10^{-6}$	Wesołowski et al. (2020b)
The refractive index for cometary ice (-)	$m_{\rm ice} = 1.31 + 0.02i$	Adopted value
The refractive index for organic matter (-)	$m_{\rm org} = 1.50 + 0.02i$	Adopted value
The refractive index for cometary dust (-)	$m_{\rm dust} = 1.60 + 0.02i$	Adopted value
The average particle radius (m)	$r = 1.96{\times}10^{-6}$	Calculated value
The effective diffraction parameter (-)	$x_{\rm eff} = 24.556$	Calculated value
The scattering efficiencies of ice water particles (-)	$Q_{\rm ice} = 1.441$	Calculated value
The scattering efficiencies of cometary dust (-)	$Q_{\rm dust} = 1.525$	Calculated value
The scattering efficiencies of organic matter (-)	$Q_{\rm org} = 1.298$	Calculated value
Asymmetry coefficient for water ice (-)	$g_{\rm ice} = 0.918$	Calculated value
Asymmetry coefficient for cometary dust (-)	$g_{\rm dust} = 0.887$	Calculated value
Asymmetry coefficient for organic matter (-)	$g_{\rm org} = 0.874$	Calculated value
The value of phase function for water ice (for phase angle $\Theta_{\rm q} = 10.06°$) (-)	$p(\Theta_{\rm q})_{\rm ice} = 1.912$	Calculated value
The value of phase function for water ice (for phase angle $\Theta_{\rm Q} = 9.21°$) (-)	$p(\Theta_{\rm Q})_{\rm ice} = 2.364$	Calculated value
The value of phase function for cometary dust (for phase angle $\Theta_{\rm q} = 10.06°$) (-)	$p(\Theta_{\rm q})_{\rm dust} = 2.114$	Calculated value
The value of phase function for cometary dust (for phase angle $\Theta_{\rm Q} = 9.21°$) (-)	$p(\Theta_{\rm Q})_{\rm dust} = 2.524$	Calculated value
The value of phase function for organic matter (for phase angle $\Theta_{\rm q} = 10.06°$) (-)	$p(\Theta_{\rm q})_{\rm org} = 2.122$	Calculated value
The value of phase function for organic matter (for phase angle $\Theta_{\rm Q} = 9.21°$) (-)	$p(\Theta_{\rm Q})_{\rm org} = 2.498$	Calculated value

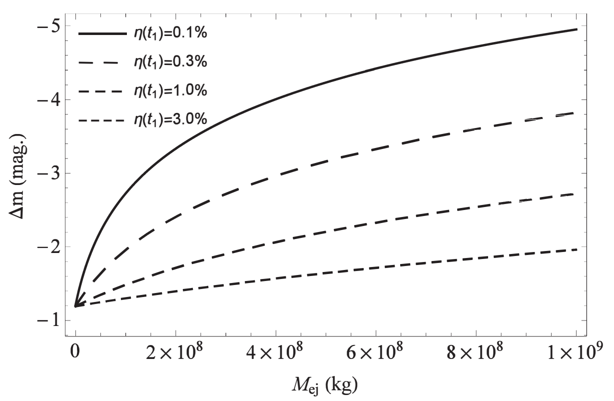

Fig. 6 Similar to Fig. 5, but scattering occurs due to ice and dust particles. In this case, in the mixture of ice and dust particles, the percentage of ice is 90%, while the dust content is 10%.

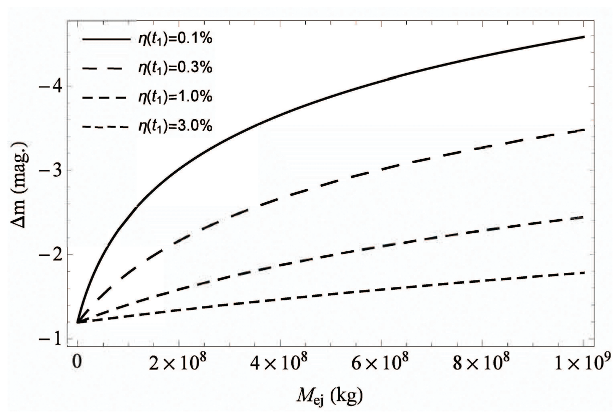

Fig. 7 Similar to Fig. 5, but in this case the percentage of ice and dust is 50%.

of subsurface layers. Another important parameter is the radius of the comet's nucleus. It turns out that it is large enough for amorphous ice to survive for a long time and up to now. The position of the comet relative to the Sun and the size of its nucleus can play important roles in explaining its unusual outburst activity by means of the thermodynamic model.

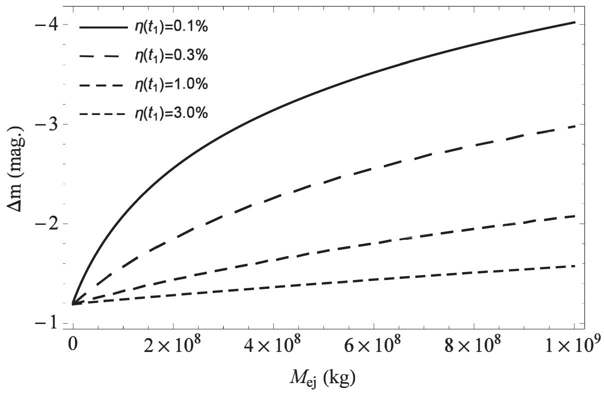

Fig. 8 Similar to Fig. 5, but in this case dust dominates, that is the percentage of dust is equal to 90% and that of ice is 10%.

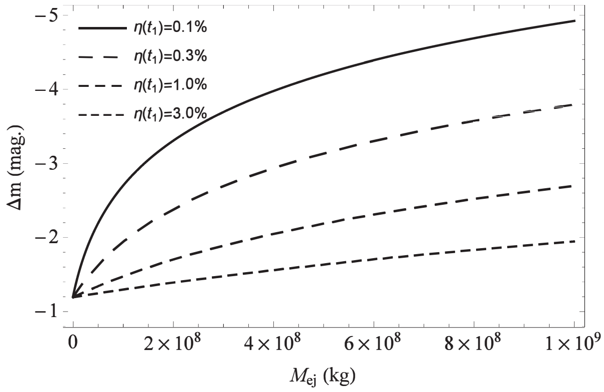

Fig. 9 Similar to Fig. 5, but scattering occurs due to ice, dust particles and organic materials. In this case, ice dominates (its percentage is 80%), the dust content is 10% and organic matter is equal to 10%.

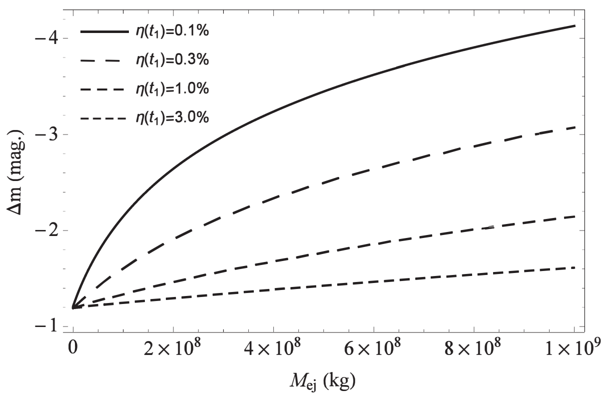

Fig. 10 Similar to Fig. 5, but dust dominates - its percentage is 80%, while the ice and dust content is equal to 10% each.

Another extremely interesting fact about comet 29P/SW is its relatively slow rotation period. For most comets, this period is measured in hours. In the case of comet 29P/SW in light of modern research, it is about 60 d.

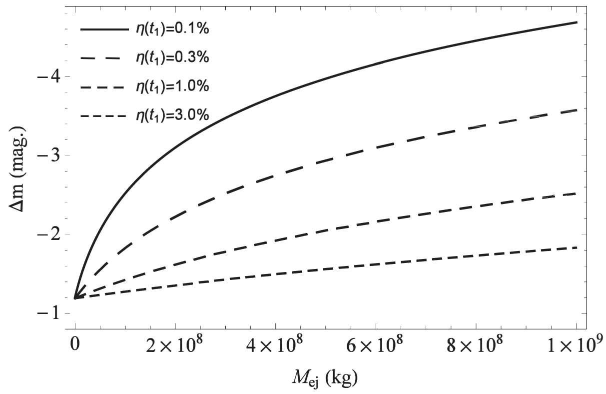

Fig. 11 Similar to Fig. 5, but organic matter dominates, its percentage is 80%, while the ice and content is 10% each.

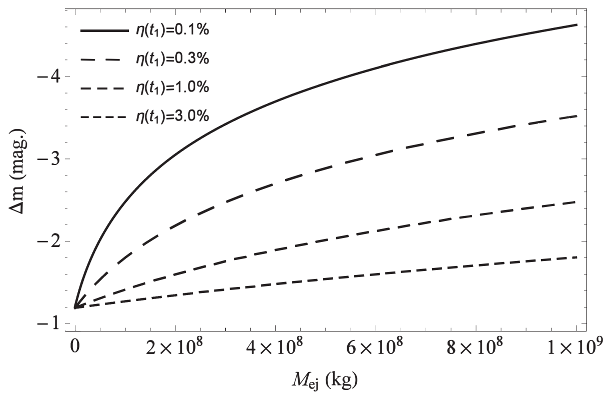

Fig. 12 Similar to Fig. 5, but scattering occurs due to ice, dust particles and organic matter, while their percentage is chosen to be equal (33.33(3)%).

In those parts of the comet that are not illuminated by the Sun during the cometary night, carbon monoxide accumulates in the cavities under the surface of the nucleus. In

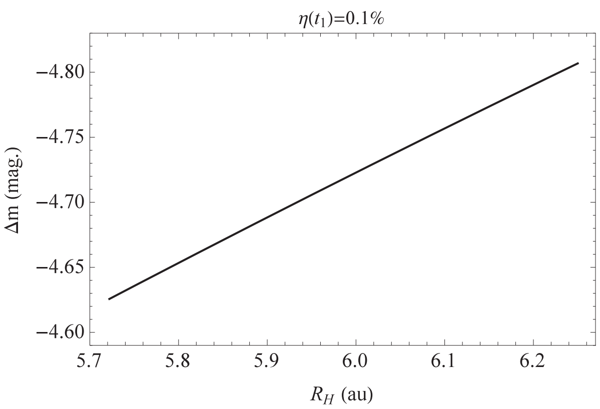

Fig. 13 The jump in cometary brightness as a function of the heliocentric distance (that is, calculated along the cometary orbit). It is assumed that the mass ejected during the outburst is equal to 10^9 kg and the active surface in the phase of quiet sublimation is equal to $\eta(t_1)$=0.1%.

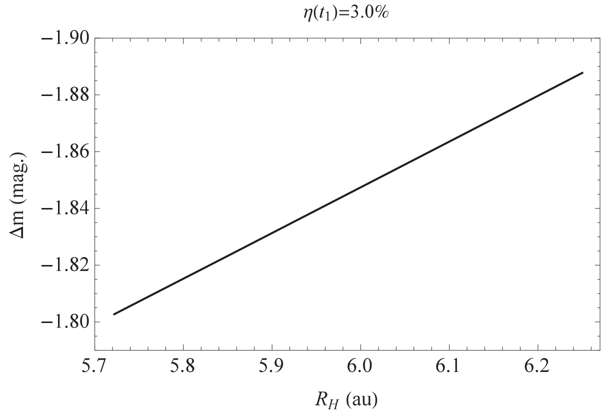

Fig. 14 Similar to Fig. 13. In the calculations, the active surface in the phase of quiet sublimation is assumed to be equal to $\eta(t_1)$=3.0%.

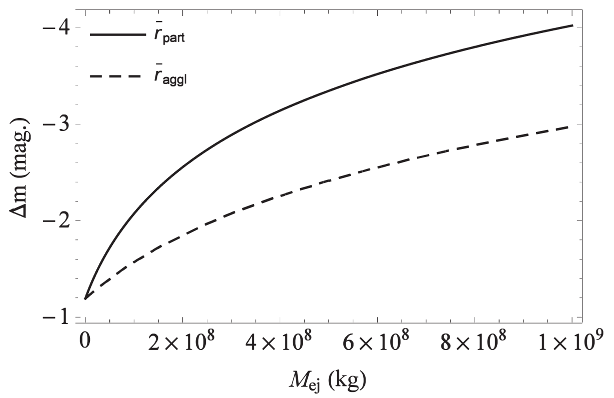

Fig. 15 The jump in comet 29P/SW brightness Δm as a function of ejected mass $M_{\rm ej}$ for two types of grains: cometary particles ($r_{\rm part}$ = 1.96 µm) and cometary agglomerates ($r_{\rm aggl}$ = 14.20 µm). In the calculations, the active surface in the phase of quiet sublimation is assumed to be equal to $\eta(t_1)$=0.1%. Comparing the obtained results, we can see that the difference between the two types of grains is about 1 magnitude. This difference depends on two key parameters: the mass ejected and the active surface in the quiet sublimation phase.

the next stage, during the comet's day, this surface is more intensively illuminated by the Sun, and it leads to a rapid expansion of gas initially trapped in the cavity. If the pressure of gas trapped in the cavity is high enough (comparable to the tensile strength of the cometary mantle), this leads to a sudden emission of cometary matter into space. That is why slow rotation and, hence, long term exposure to sunlight can contribute to weakening the cometary mantle structure. As a result, a much larger amount of cometary material can be ejected into the coma, in this way undoubtedly contributing to an effective scattering of the incident electromagnetic radiation. Then we can observe an increase in the brightness of the comet - its outburst.

As a matter of fact, the explanation of comet outbursts is not so easy, since an outburst depends primarily on the amount of mass ejected, the activity on the surface during quiet sublimation as well as during an outburst, increase in the rate of sublimation from newly exposed subsurface layers, the heliocentric distance and the type of cometary gas that was responsible for sublimation activity. All these factors were taken into account in the numerical simulations of the jump in brightness of comet 29P/SW. Above all, in our considerations, we have accounted for the presence of three types of particles in the cometary coma. They are water ice, dust and organic matter. The analysis indicates that the largest contribution comes from water ice, while the smallest from cometary dust.

It is worth noting that modern space probes (e.g., *Deep Impact* and *Rosetta*) have recorded numerous changes in brightness of comets 9P/Tempel 1 and 67P/Ch-G respectively (A'Hearn et al. 2005; Meech et al. 2005; Vincent et al. 2016; Lin et al. 2017). The analyses of their outbursts have demonstrated that most of these explosions occurred during sunrise. It means very probably that one can consider internal processes occurring within the comet nuclei by means of thermodynamic models. One of the possible approaches to the solution of the problem is presented in this paper.

In the end, we should emphasize the following: in favorable conditions, the outburst activity of 29P/SW can also be sporadically triggered by other mechanisms, such as solar wind or even collisions with large meteors. However, to the best of the author's knowledge, the only model that can explain qualitatively and quantitatively almost all features of outburst activity of 29P/SW is the thermodynamical evolution of 29P/SW.

Acknowledgements This work has been done due to the support the author received from the Centre for Innovation and Transfer of Natural Sciences and Engineering Knowledge, University of Rzeszów, Poland.

References

A'Hearn, M. F., Belton, M. J. S., Delamere, W. A., et al. 2005, Sci., 310, 258
Beer, E., Podolak, M., & Prialnik, D. 2006, Icarus, 180, 473
Beer, E., Prialnik, D., & Podolak, M. 2008, Icarus, 195, 340
Davidsson, B. J. R., & Skorov, Y. V. 2002, Icarus, 156, 223
Enzian, A., Cabot, H., & Klinger, J. 1997, A&A, 319, 995
Fanale, F. P., & Salvail, J. R. 1990, Icarus, 84, 403
Gronkowski, P., & Wesołowski, M. 2012, AN, 333, 721
Gronkowski, P., & Wesołowski, M. 2015, MNRAS, 451, 3068
Gronkowski, P., & Wesołowski, M. 2016, EM&P, 119, 23
Gronkowski, P., Tralle, I., & Wesołowski, M. 2018, AN, 339, 37

Hughes, D. W. 1991, Comets in the Post-Halley era, in Comets in the Post-Halley era, 2nd edn., eds. R. L. Newburn, M. Neugebauer, & J. Rahe (Kluwer, Dordrecht, 1991), 825

Ivanova, A. V., Afanasiev, V. L., & Korsun, P. P., et al. 2012, SoSyR, 46, 313

Kawakita, H., Watanabe, J., Ootsubo, T., et al. 2004, ApJ, 601, 191

Kolokolova, L., Hanner M. S., Levasseur-Regourd A.-Ch., et al. 2004, Comets II, M. C. Festou, H. U. Keller, and H. A. Weaver (eds.), (Tucson: University of Arizona Press), 577

Kopp G., Lean, J. L. 2011, GeoRL, 38, L01706

Kossacki, K. J., & Szutowicz, S. 2008, Icarus, 195, 705

Kossacki, K. J., & Szutowicz, S. 2013, Icarus, 225, 111

Laor, A., & Draine, B. T. 1993, ApJ, 402, 441

Lin, Z.-Y., Knollenberg, J., Vincent, J.-B., et al. 2017, MNRAS, 469, S731

Meech, K. J., Ageorges, N., A'Hearn, M. F., et al. 2005, Sci., 310, 265

Meech, K., Pittichová, J., Bar-Nun, A., et al. 2009, Icarus, 201, 719

Mishchenko, M. I., Travis L. D., & Mackowski D. W. 1996, JQSRT, 55, 535

Reach, W. T., Vaubaillon, J., Lisse, C. M., et al. 2010, Icarus, 208, 276

Miles, R. 2016, Icarus, 272, 387

Richardson, J. E., Melosh, H. J., Lisse, C. M., et al. 2007, Icarus, 190, 357

Richter, N. B. 1954, AN, 281, 241

Schambeau, C. A., Fernández, Y. R., Lisse, C. M., et al. 2015, Icarus, 260, 60

Skorov, Y., Reshetnyk, V., Lacerda, P., et al. 2016, MNRAS, 461, 3410

Stansberry, J. A., Van Cleve, J., Reach, W. T., et al. 2004, ApJS, 154, 463

Tancredi, G., Rickman, H., & Greenberg, J. M. 1994, A&A, 286, 659

Trigo-Rodriguez, J. M., García-Melendo, E., Davidsson, B. J. R., et al. 2008, A&A, 485, 599

Vincent, J. B., A'Hearn, M. F., Lin, Z.-Y., et al. 2016, MNRAS, 462, S184

Wesołowski, M., & Gronkowski, P., 2018a, NewA, 62, 55

Wesołowski, M., & Gronkowski, P., 2018b, EM&P, 121, 105

Wesołowski, M., 2019, Journal of Astrophysics and Astronomy, 40, 20

Wesołowski, M., Gronkowski, P., Tralle, I. 2019, MNRAS, 484, 2309

Wesołowski, M., Gronkowski, P., & Tralle, I. 2020a, Icarus, 338, 113546

Wesołowski, M., Gronkowski, P., & Tralle, I. 2020b, Planetary and Space Science, 184, 104867

Zubko, E., Furusho R., Kawabata K., et al. 2011, JQSRT, 112, 1848

Zubko, E. 2013, EP&S, 65, 139